Inorg. Chem. **2006**, *45*, 10355–10362

Multifrequency EPR and Redox Reactivity Investigations of a Bis(μ-thiolato)-dicopper(II,II) Complex

Wassim Rammal,[⊥] Catherine Belle,*[,⊥] Claude Béguin,[⊥] Carole Duboc,[†] Christian Philouze,[⊥] Jean-Louis Pierre,[⊥] Laurent Le Pape,[∥] Sylvain Bertaina,[§] Eric Saint-Aman,[‡] and Stéphane Torelli[⊥]

Laboratoire de Chimie Biomimétique, UMR CNRS 5616, ICMG FR CNRS 2607, BP 53X, 38041 Grenoble Cedex 9, France, Laboratoire des Champs Magnétiques Intenses, 25 Avenue des Martyrs, BP 166, 38042 Grenoble Cedex 9, France, Laboratoire de Chimie Biologique, (UMR CNRS 5047) et Laboratoire de Résonances Magnétiques, 38054 Grenoble Cedex 9, France, Laboratoire de Magnétisme Louis Néel, CNRS, BP 166, 38042 Grenoble Cedex 9, France, and Laboratoire d'Electrochimie Organique et de Photochimie Redox, UMR CNRS 5630, ICMG FR CNRS 2607, BP 53X, 38041 Grenoble Cedex 9, France

Received July 7, 2006

From a new tripodal ligand [$N_2SS'H$] with mixed N, S(thioether), and S(thiolate) donor set, the corresponding bis(μ-thiolato)dicopper(II) complex has been prepared and characterized. X-ray crystallographic analysis of the complex $[Cu_2(N_2SS')_2](ClO_4)_2 \cdot C_4H_{10}O$ (**1**) demonstrates that the two five-coordinated Cu atoms are bridged by two thiolates leading to a nearly planar Cu_2S_2 core with a Cu1···Cu1* distance of 3.418(8) Å and a large bridging angle Cu1S1Cu1* of 94.92°. X-band (10 GHz), Q-band (34 GHz), and F-Band (115 GHz) EPR spectra of **1** are consistent with a weakly coupled dicopper(II,II) center attributed to an $S = 1$ state. Simulations for the three frequencies are obtained with a unique set of electronic parameters. The mean values of the spin Hamiltonian parameters for **1** are $|D| = 0.210(3)$ cm^{-1}, $E = 0.0295(5)$ cm^{-1}, $|E/D| = 0.140$, $g_x = 2.030(2)$, $g_y = 2.032(2)$, $g_z = 2.128(2)$. The electrochemical one-electron reduction of **1** generates the mixed-valent $Cu^{II}Cu^{I}$ species. EPR and UV–vis spectra are consistent with a type I localized mixed-valent species, while dinuclear Cu_A centers of native cytochrome *c* oxidase (C*cO*)[1−3] or nitrous oxide reductase (N_2OR)[4] have a delocalized $Cu^{II}Cu^{I}$ mixed-valent state. After reoxidation of the $Cu^{II}Cu^{I}$ species, the initial complex **1** is regenerated through a reversible interconversion process.

Introduction

In the past decade, growing interest has been directed toward copper−sulfur chemistry.[5] This is related to the natural occurrence of copper−thiolate and copper−thioether bonds encountered in a wide variety of proteins[6] and particularly in redox-active proteins with electron-transfer functions. They include mononuclear type 1 blue copper proteins and dinuclear Cu_A centers from cytochrome *c* oxidase (C*cO*)[1−3] or nitrous oxide reductase (N_2OR).[4] The latter involves a dicopper unit (Figure 1) with a delocalized mixed-valent core in its resting state. The $Cu^{1.5}Cu^{1.5}$ ions are close to each other (∼2.5 Å), both in a distorted tetrahedral coordination sphere. The copper atoms are bridged by two S(Cys), leading to an essentially planar Cu_2S_2 structure. Two N(His) and two additional ligands (one S(Met) and one O carbonyl of a glutamate in C*cO*[1−3] or of a tryptophan in N_2OR[4]) in axial positions complete the coordination sphere. The purple color of the Cu_A center is

* To whom correspondence should be addressed. E-mail: Catherine.Belle@ujf-grenoble.fr
[⊥] LEDSS−Université Joseph Fourier.
[†] LCMI-CNRS, UPR 5021.
[∥] LCB-DRDC and LRM-SCIB-DRFMC, CEA Grenoble.
[§] LLN-CNRS.
[‡] LEOPR−Université Joseph Fourier.

(1) Iwata, S.; Ostermeier, C.; Ludwig, B.; Michel, H. *Nature (London)* **1995**, *376*, 660−669.
(2) Tsukihara, T.; Aoyama, H.; Yamashita, E.; Tomizaki, T.; Yamaguchi, H.; Shinzawa-Itoh, K.; Nakashima, R.; Yaono, R.; Yoshikawa, S. *Science* **1995**, *269*, 1069−1074.
(3) Wilmanns, M.; Lappalainen, P.; Kelly, M.; Sauer-Eriksson, E.; Saraste, M. *Proc. Natl. Acad. Sci. U.S.A.* **1995**, *92*, 11955−11959.
(4) Brown, K.; Tegoni, M.; Prudencio, M.; Pereira, A. S.; Besson, S.; Moura, J. G.; Moura, I.; Cambillau, C. *Nat. Struct. Biol.* **2000**, *7*, 191−195.
(5) Stiefel, E. I.; Matsumoto, K. *Transition Metal Sulfur Chemistry*; American Chemical Society: Washington, DC, 1996.
(6) Belle, C.; Rammal, W.; Pierre, J. L. *J. Inorg. Biochem.* **2005**, *99*, 1929−1936.

10.1021/ic0612606 CCC: $33.50
Published on Web 11/08/2006

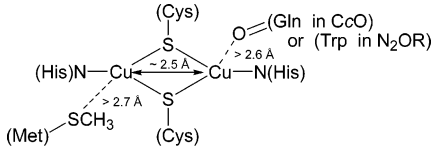

Figure 1. Schematic drawing of the Cu_A center in cytochrome *c* oxidase and nitrous oxide reductase.

Scheme 1

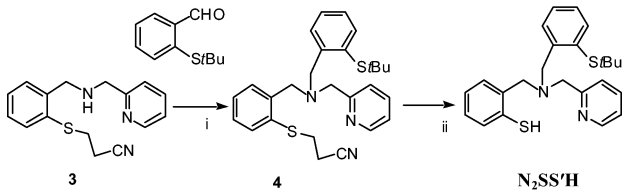

Reagents: i, $NaBH_3CN/CH_3COOH/MeOH$; ii, $MeO^-Na^+/MeOH$

the result of predominant S(Cys) → Cu charge-transfer transitions at ~480 and ~530 nm and a broad class III[7] mixed-valent charge-transfer band around ~830 nm.[8,9] The delocalized mixed-valent configuration $Cu^{1.5}Cu^{1.5}$ is consistent with the multifrequency EPR data.[10] The well-resolved seven-line pattern evidences the unpaired electron interaction with two $I = 3/2$ copper centers as described for N_2OR.[11] Both Cu_A sites allow reversible one-electron redox process ($Cu^{II}Cu^I/Cu^ICu^I$) at a potential around +240 mV.[12,13]

Interestingly, a four-line EPR hyperfine structure, typical of a localized valence has been observed at pH = 4.0 for an engineered Cu_A center in azurin.[14]

Only a few examples of dinuclear complexes containing thiolate bridges between $Cu^{II}Cu^I$ [15] or $Cu^{II}Cu^{II}$ [16−19] have been reported so far. In addition, the electrochemistry and the magnetic properties of these complexes have not extensively been studied. To further explore the properties of such copper species, we have prepared and characterized a bis(μ-thiolato)dicopper(II) complex from a new tripodal ligand [$N_2SS'H$] (Scheme 1). Complex $[Cu_2(N_2SS')_2](ClO_4)_2 \cdot C_4H_{10}O$ (**1**) represents a unique example of stable dithiolate-bridged dinuclear Cu^{II} complex with a mixed thiolate and thioether coordination around the copper centers. Furthermore, the preparation of the mixed-valent state has been explored for a better understanding of the factors controlling the redox conversion.

Results and Discussion

Synthesis. Formation of a Cu^{II}−thiolate bond competes with the normally favored redox reaction [$2RS^- + 2Cu^{II} \leftrightarrows RSSR + 2Cu^I$].[20] Destabilization of the redox reaction is achieved herein by using a new ligand ([$N_2SS'H$], Scheme 1) that sterically (*tert*-butyl group) precludes the reaction of two mercaptides at the copper center. Moreover, aromatic thiolate is stabilized by charge delocalization.

The synthetic route for the preparation of the tripodal ligand [$N_2SS'H$], which bears three different arms, is depicted in Scheme 1. Precursor **3** is obtained as previously described[21] from thiosalicylic acid after protection of the thiolate function in order to avoid its oxidation. Further condensation of **3** with 2-(*tert*-butylthio)benzaldehyde and reductive amination in MeOH using $NaBH_3CN$ affords the tertiary amine **4** with one *tert*-butyl- and one cyanoethyl-protected thiolate arm (80% yield). Selective deprotection of the cyanoethyl group using sodium methanolate in MeOH affords after workup the pure thiolate ligand [$N_2SS'H$] (98% yield) with one S(thiolate) and one S(thioether) donor.

The $Cu^{II}Cu^{II}$ complex from the ligand [$N_2SS'H$] is obtained by mixing a stoichiometric amount of $Cu(ClO_4)_2 \cdot 6H_2O$ to a solution of the ligand in methanol. Upon addition of diethyl ether, the crude product precipitates as a black powder. Recrystallization affords pure **1** as black-purple crystals of X-ray quality with diethyl ether as solvate. The solid compound is air stable for months at room temperature, as well as in solution (dichloromethane at −20 °C). The electrospray ionization mass spectrum of a dichloromethane solution of **1** provides prominent peaks at the expected mass numbers with the distribution patterns of the corresponding dicopper(II) complex (Figure S1 in the Supporting Information), suggesting that the dimeric structure remains in solution. In dichloromethane solution, the electronic spectrum reveals two transitions at 350 ($\epsilon = 7158\ M^{-1}\ cm^{-1}$) and 592 nm ($\epsilon = 1204\ M^{-1}\ cm^{-1}$). These features are in the range of those reported for pentacoordinated bis(μ-thiolato) dicopper(II) complexes at 350−382 nm ($\epsilon \approx 3600-11\,000\ M^{-1}\ cm^{-1}$) together with one or two broad bands around 500−676 ($\epsilon \approx 120-670\ M^{-1}\ cm^{-1}$) and 810−880 nm ($\epsilon \approx 1200\ M^{-1}\ cm^{-1}$).[16,17]

Description of crystal structure for 1. The cationic unit shown in Figure 2 consists of two five-coordinated Cu atoms bridged by two thiolate groups. The dicationic molecular entity possesses a 2-fold symmetry axis passing through the midpoint of Cu1···Cu1* axis and the μ-thiolato bridge. Only half a molecular unit is thus crystallographically defined. Selected bond distances and angles are listed in Table 1.

(7) Robin, M. B.; Day, P. *Adv. Inorg. Chem. Radiochem.* **1967**, *10*, 247−422.
(8) Farrar, J. A.; Neese, F.; Lappalainen, P.; Kroneck, P. M. H.; Saraste, M.; Zumft, W. G.; Thomson, A. J. *J. Am. Chem. Soc.* **1996**, *118*, 11501−11514.
(9) Kroneck, P. M. H. In *Handbook of metalloproteins*; Wiley: New York, 2001; pp 1333−1341.
(10) Antholine, W. E.; Kastrau, D. H. W.; Steffens, G. C. M.; Zumft, W. G.; Kroneck, P. M. H. *Eur. J. Biochem.* **1992**, *209*, 875−881.
(11) Neese, F.; Zumft, W. G.; Antholine, W. A.; Kroneck, P. M. H. *J. Am. Chem. Soc.* **1996**, *118*, 8692−8699.
(12) Coyle, C. L.; Zumft, W. G.; Kroneck, P. M. H.; Körner, H.; Jakob, W. *Eur. J. Biochem.* **1985**, *153*, 459−467.
(13) Lappalainen, P.; Aasa, R.; Malmström, B. G.; Saraste, M. *J. Biol. Chem.* **1993**, *268*, 26416−26421.
(14) Hwang, H. J.; Lu, Y. *Proc. Natl. Acad. Sci. U.S.A.* **2004**, *101*, 12842−12847.
(15) Houser, R. P.; Young, J., V. G.; Tolman, W. B. *J. Am. Chem. Soc.* **1996**, *118*, 2101−2102.
(16) Houser, R. P.; Halfen, J. A.; Young, V. G., Jr.; Blackburn, N. J.; Tolman, W. B. *J. Am. Chem. Soc.* **1995**, *117*, 10745−10746.
(17) Itoh, S.; Nagagawa, M.; Fukuzimi, S. *J. Am. Chem. Soc.* **2001**, *123*, 4087−4088.
(18) Ueno, Y.; Tachi, Y.; Itoh, S. *J. Am. Chem. Soc.* **2002**, *124*, 12428−12429.
(19) Brandscombe, N. D. J.; Blake, A. J.; Marin-Becerra, A.; Li, W.; Parsons, S.; Ruiz-Ramirez, L.; Schröder, M. *Chem. Comm.* **1996**, 2573−2574.
(20) Hemmerich, P.; Beinert, H.; Vänngard, T. *Angew. Chem., Int. Ed. Engl.* **1966**, *5*, 422−423.
(21) Belle, C.; Bougault, C.; Averbuch, M. T.; Durif, A.; Pierre, J. L.; Latour, J. M.; Le Pape, L. *J. Am. Chem. Soc.* **2001**, *123*, 8053−8066.

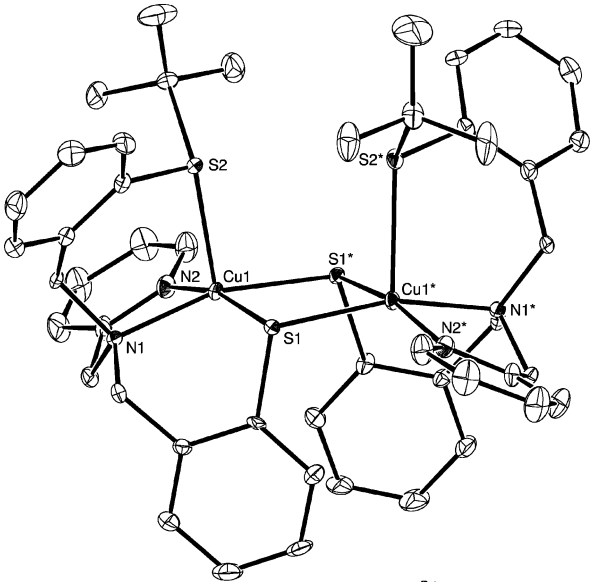

Figure 2. ORTEP drawing of the cationic unit $[Cu_2(N_2SS')_2]^{2+}$ showing the 25% probability thermal ellipsoids. Hydrogens are omitted for clarity.

Table 1. Selected Bond Distances (Å) and Angles (deg) for $[Cu_2(N_2SS')_2](ClO_4)_2{\cdot}C_4H_{10}O$[a]

Cu1−S1	2.318(1)	Cu1−N2	2.025(3)
Cu1−S1*	2.322(1)	Cu1···Cu1*	3.4185(8)
Cu1−S2	2.554(1)	S1···S1*	3.130(2)
Cu1−N1	2.077(3)		
Cu1−S1−Cu1*	94.92(4)	S1−Cu1−N2	166.1(1)
S1−Cu1−S1*	84.84(4)	S2−Cu1−N1	96.36(9)
S1−Cu1−S2	85.87(3)	S2−Cu1−N2	107.5(1)
S1−Cu1−N1	92.53(9)	N1−Cu1−N2	82.2(1)

[a] Symmetry operation: $-x, +y, 0.5 - z$.

Each copper center is in a distorted square pyramidal geometry (a deviation of −0.2986(1) Å from the mean plane N1N2S1S1* around the copper atom is observed). The coordination sphere of Cu1 is achieved by the thiolate arms from two ligands (S1 and S1*), two nitrogen atoms from amino (N1) and pyridyl (N2) groups, and in apical position the thioether sulfur atom (S2). The two Cu−S(thioether) bonds are on the same side of the Cu_2S_2 core. The dihedral angle between the N1N2S1S1* and N1*N2*S1S1* planes is ca. 167°. In the Cu_2S_2 core, the atoms are almost coplanar with a dihedral angle between the S1Cu1S1*/S1Cu1*S1* planes of 172.89° (distortion of the Cu_2S_2 cores along the S1−S1* axis about 7°). Furthermore, a large bridge angle Cu1S1Cu1* is observed (94.92°). In contrast, previously described pentacoordinated bis(μ-thiolato)dicopper(II) complexes display a distortion of the Cu_2S_2 core along the S−S axis about 33.5°[16] and 36°[17] evidencing a distinct "butterfly" core with smaller bridging CuSCu angles (91.52°,[16] 80.95°, and 79.6°,[17] respectively). As a consequence, the intermetallic distance in **1** (3.418(8) Å) is significantly longer compared to other reported distances in pentacoordinated bis(μ-thiolato)dicopper(II) complexes (2.96,[17] 3.264(2), and 3.340(3) Å[16]). The Cu_2S_2 unit in **1** is slightly asymmetric, as indicated by nearly equal bond distances (Cu1−S1 = 2.318(1) and Cu1−S1* = 2.322(1) Å, respectively) of the bridging sulfur atoms. These Cu−S(thiolate) distances fall in the same range as the previously described compounds.[16,17,19]

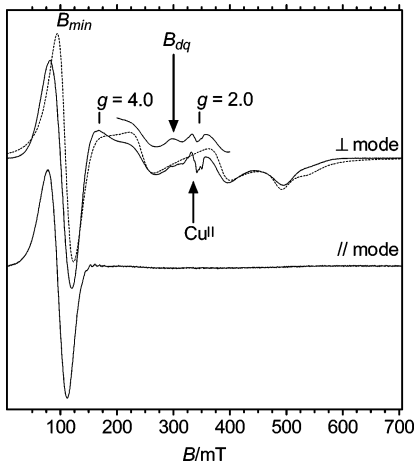

Figure 3. X-band EPR spectra of $[Cu_2(N_2SS')_2](ClO_4)_2{\cdot}C_4H_{10}O$ (**1**) in CH_2Cl_2 (∼8 mM) under argon at 10 K. Perpendicular mode (top), experimental (—), microwave frequency, 9.65401 GHz; microwave power, 0.80 mW; modulation frequency, 100 kHz; modulation amplitude, 1.04 mT, one scan, 336 s; saturated portion (200−400 mT), same parameters except microwave frequency, 9.65403 GHz; microwave power, 13 mW; simulation (···) with $|D| = 0.212$ cm^{-1}, $E = 0.0295$ cm^{-1}, $g_x = 2.030$, $g_y = 2.032$ $g_z = 2.128$, $W_x = 20$ mT, $W_y = 35$ mT and $W_z = 20$ mT. Parallel mode (bottom), same parameters except microwave frequency, 9.38949 GHz and microwave power, 0.80 mW.

The Cu−S(thioether) apical bonds (2.554(1) Å) are longer than the usual Cu^{II}−S(thioether) distances (average 2.42(14) Å) reported for $Cu-SR_2$ complexes.[22] As expected, the Cu−N interaction for tertiary amine (Cu−N1 = 2.077 (3) Å) is weaker relative to pyridine amine (Cu−N2 = 2.025 (3) Å).

EPR Studies. EPR properties of **1** have been investigated at different microwave frequencies, both in the polycrystalline state and in frozen solution.

EPR Spectra. X-band EPR spectra of a CH_2Cl_2 frozen solution of **1** recorded both in perpendicular and parallel modes are shown in Figure 3. In polycrystalline state, similar spectra and properties are observed (Figure S2 in Supporting Information), except for some orientation effects and shapes and intensities of the signals corresponding to the Cu^{II}-type components observed between 270 and 360 mT.[23] This indicates that the solid-state structure of the dinuclear compound is preserved in CH_2Cl_2 solution. Measurements up to 905 mT strengthen that signals extend from 0 to ca. 700 mT.

In perpendicular mode, the X-band EPR spectrum is dominated by an intense unresolved line located in the 20−160 mT region, centered at $g \approx 6.8$, which could be initially attributed mostly to a "forbidden" $\Delta M_S = \pm 2$ transition (B_{min}) (absorption of one photon inducing a transition between the $M_S = -1$ and $+1$ levels). In parallel mode, the observation of this unique and intense unresolved line at about $g \approx 7.0$

(22) Ambundo, E. A.; Deydier, M. V.; Grall, A. J.; Aguera-Vega, N.; Dressel, L. T.; Cooper, T. H.; Heeg, M. J.; Ochrymowycz, L. A.; Rorabacher, D. B. *Inorg. Chem.* **1999**, *38*, 4233−4242.

(23) These signals saturate more easily than the rest of the spectrum. At 10 K, the power should be as low as 0.20 mW to be out of saturation. Measurements from 5 up to 80 K show a Curie law variation of the intensity of this part of the spectrum. These properties are consistent with the presence of at least two Cu^{II} species as uncoupled, dinuclear species or mononuclear ones.

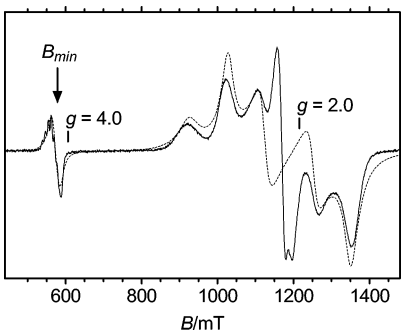

Figure 4. Q-band EPR spectra of $[Cu_2(N_2SS')_2](ClO_4)_2 \cdot C_4H_{10}O$ (**1**) in CH_2Cl_2 under helium at 13 K: experimental (—), microwave frequency, 33.9490 GHz; microwave power, 2.86 μW; modulation frequency, 100 kHz; modulation amplitude, 0.48 mT; one scan, 336 s; simulation (···) with $|D| = 0.212$ cm^{-1}, $E = 0.0295$ cm^{-1}, $g_x = 2.030$, $g_y = 2.034$ $g_z = 2.128$, $W_x = 20$ mT, $W_y = 35$ mT, and $W_z = 20$ mT.

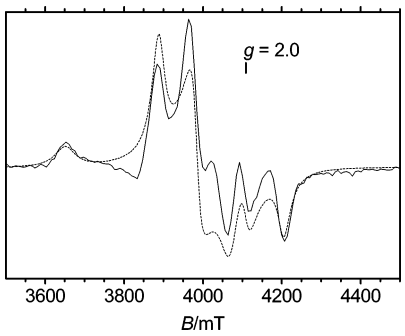

Figure 5. F-band EPR spectra of $[Cu_2(N_2SS')_2](ClO_4)_2 \cdot C_4H_{10}O$ (**1**) in CH_2Cl_2 under helium at 10 K: experimental (—), microwave frequency, 115 GHz; modulation amplitude, 0.30 mT; simulation (···) with $|D| = 0.207$ cm^{-1}, $E = 0.0295$ cm^{-1}, $g_x = 2.030$, $g_y = 2.030$ $g_z = 2.128$, $W_x = 20$ mT, $W_y = 35$ mT, and $W_z = 20$ mT.

is the signature of a non-Kramers system in agreement with a triplet spin state.[24,25] The saturation properties of this line are similar to those of a line observed between 270 and 320 mT ($g \approx 2.24$) at higher microwave power (13 mW in Figure 3). Both are less sensitive to saturation effects than the other components of the triplet spin state spectrum. This second line could be attributed to a double quantum transition (B_{dq}) which corresponds to two microwave quanta that may be absorbed for the complexes oriented such that the $M_S \pm 1$ levels are separated from the $M_S = 0$ level by $h\nu$.[26]

The other lines are out of saturation at 0.80 mW at 10 K. The shape of the triplet spin state spectra does not change between 4 and 20 K, slightly varies at 40 K, and then significantly varies at 80 K. Changes correspond to a closing of the lines around $g \approx 2$, which indicates a decrease of zero-field splitting. This temperature effect on the zero-field splitting is explained by slight structural modifications around the Cu^{II} ion.[27] Line width does not vary up to 80 K. A Curie-like behavior is observed from 4.2 to 40 K (isotropic spin−spin interaction $|J_0| < 1$ cm^{-1}). These properties are consistent with a weakly coupled dicopper(II,II) center with $S = 1$.

The dinuclear Cu^{II} complex **1** was also investigated by EPR at Q-band (Figure 4) in polycrystalline state and in a frozen dichloromethane solution. Both spectra are similar, but the polycrystalline spectra are less resolved around B_{min}, with a slightly larger zero-field splitting, and display some orientation effects and different intensities at g values slightly higher than 2 (Figure S3 in Supporting Information). The increase of the zero-field splitting is in accordance with a more compact structure in solid state than in frozen solution. The lines at $g \approx 4.23$ and another one with a maximum at ca. 1157 mT and a minimum at ca. 1187 mT are less sensitive to saturation. They can be attributed to B_{min} and B_{dq} transitions, respectively. The other two lines between 1130 and 1230 mT could be tentatively attributed to Cu^{II} species. The resonance at B_{min} is resolved with seven hyperfine lines separated by ca. 8.1 mT. They are due to two interacting Cu^{II} with $I = 3/2$. This kind of splitting in the $\Delta M_S = \pm 2$ transition has already been observed in other X-band EPR spectra of dicopper(II,II) complex.[28,29] The other lines follow a Curie-like behavior between 13 and 100 K. These properties are also consistent with a weakly coupled dicopper(II,II) compound with $S = 1$.

Table 2. Spin Hamiltonian Parameters Derived by Simulation for **1** at Different Frequencies

	$\|D\|$ cm^{-1}	E cm^{-1}	$\|E/D\|$	g_x	g_y	g_z
X-band	0.212	0.0295	0.139	2.030	2.032	2.128
Q-band	0.212	0.0295	0.139	2.030	2.034	2.128
F-band	0.207	0.0295	0.142	2.030	2.030	2.128

The dinuclear Cu^{II} complex **1** was also investigated by EPR at 115 GHz (F-band) (Figure 5) in a frozen dichloromethane solution. At F-band, the only transitions observed in the spectrum between 3600 and 4400 mT originate from $\Delta M_S = \pm 1$ triplet spin transitions. At this frequency, high field limit conditions are reached since the energy provided by the EPR spectrometer (3.8 cm^{-1}) is higher than the magnitude of D. In those conditions, the field difference (440 mT) between two z transitions is equal to $2D/\mu_B g_z$. The magnitude of the zero-field splitting can therefore be estimated as $|D| = 220$ mT (0.218 cm^{-1}).

Simulation and Analysis of the EPR Spectra. To determine the spin Hamiltonian parameters, simulations have been performed with the SIM program[30] using the spin Hamiltonian (eq 1) considering collinear $\tilde{g}$ and $\tilde{D}$ tensors.

$$H_S = \mu_B \vec{B} \cdot \tilde{g} \cdot \hat{S} + \hat{S} \cdot \tilde{D} \cdot \hat{S} \qquad (1)$$

Simulated X-band, Q-band, and F-band EPR spectra are shown in Figures 3, 4, and 5, respectively, and the corresponding spin Hamiltonian parameters used are reported in Table 2.

As can be seen, the three sets of parameters are similar for the three frequencies. We can thus propose that the spin

(24) Weltner, W. *Magnetic atoms and molecules*; Dover Publication: New York, 1983; Chapter III, p 165.
(25) Le Pape, L.; Belle, C.; Duboc, C.; Béguin, C.; Pierre, J. L. Unpublished results.
(26) de Groot, M. S.; van der Waals, J. H. *Physica* **1963**, *29*, 1128−1132.
(27) Dyrek, K.; Goslar, J.; Hodorowicz, S. A.; Hoffmann, S. K.; Oleksyn, B. J.; Weselucha-Birczynska, A. *Inorg. Chem.* **1987**, *26*, 1481−1487.
(28) Pierre, J. L.; Chautemps, P.; Refaif, S.; Beguin, C.; El Marzouki, A.; Serratrice, G.; Saint-Aman, E.; Rey, P. *J. Am. Chem. Soc.* **1995**, *117*, 1965−1973.
(29) Spencer, D. J. E.; Reynolds, A. M.; Holland, P. L.; Jazdzewski, B. A.; Duboc-Toia, C.; Le Pape, L.; Yokota, S.; Tachi, Y.; Itoh, S.; Tolman, W. B. *Inorg. Chem.* **2002**, *41*, 6307−6321.
(30) Glerup, J.; Weihe, H. *Acta Chem. Scand.* **1991**, *45*, 444−448.

Hamiltonian parameters for **1** correspond to their mean value: $|D| = 0.210(3)$ cm^{-1}, $E = 0.0295(5)$ cm^{-1}, $|E/D| = 0.140$, $g_x = 2.030(2)$, $g_y = 2.032(2)$, $g_z = 2.128(2)$.

The magnitude of the axial zero field splitting determined for **1** falls in the range [0−1.41 cm^{-1}] reported in the literature for dibridged dicopper(II,II) complexes.[31−33] However, even with measurements performed at low temperature and at 115 GHz, the sign of D was not determined since no significant change in the relative intensities of the different lines has been observed. The magnitude of D is small enough for all Zeeman levels to be populated at the lowest temperature used.

The simulation allows us to definitively attribute the transitions of the triplet spin state. For X-band spectra, the simulation shows that the intense $g \approx 6.8$ signal corresponds to the contribution of different transitions that superimpose two $\Delta M_S = \pm 2$ transitions ($|1,-1\rangle \rightarrow |1,+1\rangle$) along x and y[25] but also two $\Delta M_S = \pm 1$ transitions along y and z. This overlap is strongly related to a particular D/ν value (around 0.66) as shown in Figure S4 (Supporting Information). The two $\Delta M_S = \pm 1$ along x are located at 220 and 390 mT, the second y and z at 500 and 560 mT, respectively. The dominant line, observed in X-band, shows a decrease in intensity in Q-band and vanishes in F-band since the relative intensity of the $\Delta M_S = \pm 2$ transition compared to the $\Delta M_S = \pm 1$ transition decreases when the EPR frequency increases.[25,34,35] For Q-band, the six $\Delta M_S = \pm 1$ transitions are located at 924 (z), 1024 (y), 1124 (x), 1250 (x), 1350 (y), and 1370 mT (z). At F-band frequency, these transitions are observed between 3600 and 4400 mT: 3640 (z), 3890 (y), 3980 (x), 4080 (z), 4120 (x), and 4210 mT (y).

To confirm the attribution of the double-quantum transition, which was not simulated, its field position has been calculated according to a previously reported formula.[26] At X- and Q-band, using the parameters mentioned in Figures 3 and 4, calculation gives $B_{dq} = 308$ and 1170 mT, respectively. These values correspond to the position of the experimental lines previously attributed to B_{dq}. At F-band, this transition could not be ascertained. However, calculation gives $B_{dq} = 3980$ mT, which is overlapped under the triplet state line (Figure 5).

These overall EPR studies unambiguously show that the observed EPR signals correspond to a triplet spin state with a weak isotropic part, J_0, of the spin−spin interaction. However, simulations considering a triplet state are valid only if some conditions are respected: the hyperfine coupling and the Dzyaloshinsky−Moriya term should be negligible. It is true for complex **1** since $a_{iso} < 7\ 10^{-3}$ cm^{-1} and the antisymmetric anisotropic part of the spin−spin interaction is zero with the presence of a C_2 axis in **1** ($\tilde{g}_{Cu1} = \tilde{g}_{Cu1*}$ considering both tensors collinear). Furthermore, $|\Delta g_i \mu_B B|$, where Δg_i are the three components $i = x, y, z$ of the tensor $\Delta\tilde{g} = \tilde{g}_{Cu1} - \tilde{g}_{Cu1*}$, should be small compare to $|D_i|$, where D_i are the three components i of the zero-field splitting tensor, $\tilde{D}$, the symmetric anisotropic part of the spin−spin coupling.[36] As $\Delta g_i = 0$, this condition is also followed.

Could singlet−triplet spin-state mixing invalidate our methodology, especially considering the small isotropic spin−spin coupling observed? We have compared simulated spectra at X-, Q-, and F-band frequencies considering two different approaches, with exact diagonalization of the respective full Hamiltonian, with the same set of parameters g_i and D_i, taking those deduced from Table 2 at X-band as an example. The first Hamiltonian (eq 1) corresponds to an $S = 1$ system (i.e., the triplet state of two Cu^{II} ions with an infinite isotropic spin−spin interaction). The second Hamiltonian (eq 2) describes the system as two Cu^{II} ions ($S = 1/2$), with an isotropic spin−spin interaction close to zero ($J_0 = -2 \times 10^{-4}$ cm^{-1}):

$$H_S = \mu_B \vec{B}\cdot\tilde{g}_{Cu1}\cdot\hat{S}_1 + \mu_B \vec{B}\cdot\tilde{g}_{Cu1*}\cdot\hat{S}_2 + \hat{S}_1\cdot\tilde{J}\cdot\hat{S}_2 \qquad (2)$$

with $S_1 = S_2 = 1/2$, $\tilde{g}_{Cu1} = \tilde{g}_{Cu1*} = \tilde{g}$, and $\tilde{J} = J_0 + 2\tilde{D}$. The factor 2 corresponds to the normalization factor, $S(S + 1)$, allowing comparison between zero-field splitting parameters obtained in the $S = 1$ description and in the two $S = 1/2$ description. Simulations using a large line width (15 mT), as observed in the experimental spectra, show no detectable differences between the two methods (Figures S5−7 in Supporting Information). Differences (thin lines at $g \approx 2$) can only be observed with small line width (1 mT) (Figures S8−10 in Supporting Information).

Concerning the apparent shift of the effective zero-field splitting at F-band frequency, deviations from the observed crystallographic symmetry could be invoked. Taking for example $|\Delta g_i|$ of the order of 10^{-3},[37] a small effect is expected at F-band frequency on the lines located at the highest field. A little deviation from the exact collinearity of the tensors can also be proposed. We have checked that if the two g_z directions of the intrinsic $\tilde{g}$ tensors are slightly different, some effects can be observed only at F-band.

The small isotropic spin−spin interaction may be rationalized upon considering that the ferromagnetic and antiferromagnetic contributions to this interaction may compensate each other.[38,39] In the bis(μ-hydroxo)dicopper(II) complexes series, the studies of Hatfield et al.,[40] showed that this situation occurs for a CuOCu bridge angle of 97.5°. In **1**,

(31) Hathaway, B. J. *Comprehensive Coordination Chemistry*; Wilkinson, S. R., Gillard, R. D., M Cleverty, J. A., Eds.; Pergamon Press: Oxford, 1987; Vol. 5, pp 662−673.
(32) Banci, L.; Bencini, A.; Gatteschi, D. *J. Am. Chem. Soc.* **1983**, *105*, 761−764.
(33) Gutiérrez, L.; Alzuet, G.; Borras, J.; Castineiras, A.; Rodriguez-Fortea, A.; Ruiz, E. *Inorg. Chem.* **2001**, *40*, 3089−3096.
(34) Eaton, S. S.; More, K. M.; Sawant, B. M.; Eaton, G. R. *J. Am. Chem. Soc.* **1983**, *105*, 6560−6567.
(35) Sapina, F.; Burgos, M.; Escriva, E.; Folgado, J. V.; Beltran, D.; Gomez-Romero, P. *Inorg. Chim. Acta* **1994**, *216*, 185−190.
(36) Fournel, A.; Gambarelli, S.; Guigliarelli, B.; More, C.; Asso, M.; Chouteau, G.; Hille, R.; Bertrand, P. *J. Chem. Phys.* **1998**, *109*, 10905−10913.
(37) The two most similar Cu^{II}-type EPR spectra observed after monoelectronic reduction can be assigned to the two expected mixed-valent dicopper(II,I). The corresponding $|\Delta g'_i|$ is of the order of 10^{-2}, a value corresponding to slightly different copper sites. With $|\Delta g_i| = 10^{-3}$ cm^{-1}, $|\Delta g_i \mu_B B| \approx 2 \times 10^{-4}$, 7×10^{-4}, and 2×10^{-3} cm^{-1}, for the line at the highest field, at X-, Q-, and F-band frequencies, respectively. As the smallest possible value for $|D_i|$ is 4×10^{-2} cm^{-1}, the last condition is still valid at least at X-band and Q-band frequencies.
(38) Hay, P. J.; Thibeault, J. C.; Hoffmann, R. *J. Am. Chem. Soc.* **1975**, *97*, 4884−4899.

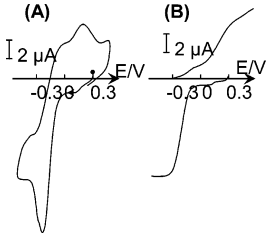

Figure 6. (A) Voltammetric curve for $[Cu_2(N_2SS')_2](ClO_4)_2 \cdot C_4H_{10}O$ (**1**) in CH_2Cl_2(1 mM) + TBAP 0.1 M. (B) Voltammetric curves (RDE) (0.08 mM) in CH_2Cl_2 + TBAP 0.1 M, V vs $Ag/AgNO_3$ 10 mM.

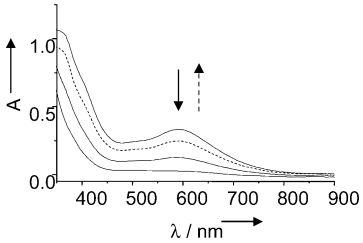

Figure 7. UV−vis spectra during exhaustive reduction at −0.4 V of $[Cu_2(N_2SS')_2](ClO_4)_2 \cdot C_4H_{10}O$ (**1**) (4 mM) in CH_2Cl_2 + TBAP (0.1 M) for $n = 0$, 0.5 and 1.00 exchanged electron (—) and reoxidized species at one electron exchanged (· · ·).

the corresponding Cu1S1Cu1* bridge angle amounts to 94.9° which is indeed in the same range. As shown by Rojo et al.,[41] the more diffuse character of the sulfur orbitals lead to a higher overlap and a stronger antiferromagnetic contribution to the isotropic spin−spin interaction than oxygen-bridged systems. On the other hand, the ferromagnetic component related to the electron exchange is not likely to be significantly different between O- and S-bridged species. As a consequence of the intrinsically higher overlap, a smaller bridge angle will be necessary in the thiolato-bridged species to compensate the ferromagnetic contribution, therefore explaining the angular difference between the O- and S-bridged complexes. Thus, the small value of the Cu1S1Cu1* angle probably lies in the range where the antiferromagnetic and ferromagnetic contributions cancel each other, leading to an overall very weak isotropic spin−spin interaction.

The compounds previously reported by Tolman[16] and Itoh[17] are EPR silent (X-Band), suggesting that the two copper atoms are strongly antiferromagnetically coupled. However, for the complex described by Tolman, a recent study indicates an $S = 1$ ground spin state based on temperature-variable field MCD measurements.[42]

Electrochemistry and the Mixed-Valent $Cu^{II}Cu^{I}$ Core Formation. The electrochemical properties of **1** have been studied by cyclic voltammetry in dichloromethane solution, as well as the corresponding electrogenerated mixed-valent species (V vs $Ag/AgNO_3$ 10 mM). When scanning toward the negative region of potentials, the CV curve is characterized by two successive reversible electrochemical signals (Figure 6A), partially overlapped and of different intensities. Further cathodic reduction of the complex leads to its decomposition accompanied by the deposition of metallic copper onto the electrode surface. The first electrochemical signal, at $E_{1/2} = +0.24$ V, is much weaker than the second one at −0.22 V. Accordingly, the voltammogram recorded at the rotating disk electrode (RDE, Figure 6B) displays two successive cathodic waves at $E_{1/2} = +0.24$ and −0.22 V, respectively, whose intensities are in a $I_{-0.22}/I_{0.24}$ ratio close to 15. Coulometric titration by potentiostatic exhaustive electrolysis performed at the potential $E = -0.4$ V gives

Scheme 2

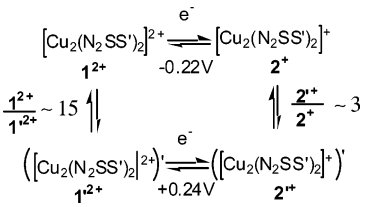

$n = 1$ exchanged electron per complex for the overall process. The resulting RDE voltammogram is characterized by two successive anodic waves corresponding to the two electrochemical systems described above. However, the $I_{-0.22}/I_{0.24}$ intensity ratio is now of ca. 3. All together, these results can be rationalized from the following square Scheme 2.

The initial $Cu^{II}Cu^{II}$ complex is in equilibrium with another $Cu^{II}Cu^{II}$ complex denoted **1′**$^{2+}$ $([Cu_2(N_2SS')_2]^{2+})'$ characterized by a change in the coordination mode of the copper centers.

As determined from the RDE wave intensities, a value close to 15 can be estimated for the corresponding equilibrium constant.

The one-electron reduction of these species leads to the corresponding mixed-valent $Cu^{II}Cu^{I}$ complexes **2**$^{+}$ and **2′**$^{+}$ $([Cu_2(N_2SS')_2]^{+}$ and $([Cu_2(N_2SS')_2]^{+})'$, respectively, which are also in equilibrium with a constant close to 3. During electrolysis, the color of the solution changes from dark purple to light brown. The corresponding UV−vis spectra were recorded (Figure 7), showing the progressive decrease in absorption at 350 and 592 nm. These bands do not completely disappear and are slightly shifted (256 and 631 nm, respectively) after one exchanged electron accounting for the remaining charge transfer and d−d absorption of the mixed-valent species. The UV−vis features of the reoxidized species are close to the initial oxidized compound **1**, indicating an almost quantitative conversion.

One-electron reduction and reoxidation of **1** has also been followed by X-band EPR in the frozen solution of CH_2Cl_2 and in the presence of the electrolyte used for the electrochemical experiments, as showed in Figure 8. After reduction (spectrum b), all the lines corresponding to the dicopper(II,II) species disappeared. The signals observed correspond to two Cu^{II}-type species at least. They could be attributed to localized mixed-valent dicopper(II,I) or mononuclear Cu^{II} species.[43] Reoxidation of this sample gives spectrum c. The signal corresponds to the $S = 1$ coupled dicopper(II,II) species observed in the initial state. As judged from a lower

(39) Kahn, O. *Molecular Magnetism*; VCH: New York, 1993.
(40) Crawford, V. H.; Richardson, H. W.; Wasson, J. R.; Hodgson, D. J.; Hatfield, W. E. *Inorg. Chem.* **1976**, *15*, 2107−2110.
(41) Garcia-Tojal, J.; Urtiaga, M. K.; Cortes, R.; Lezama, L.; Arriortua, I. M.; Rojo, T. *J. Chem. Soc., Dalton Trans.* **1994**, 2233−2238.
(42) Gamelin, D. R.; Randall, D. W.; Hay, M. T.; Houser, R. P.; Mulder, T. C.; Canters, G. W.; de Vries, S.; Tolman, W. B.; Lu, Y.; Solomon, E. I. *J. Am. Chem. Soc.* **1998**, *120*, 5246−5263.

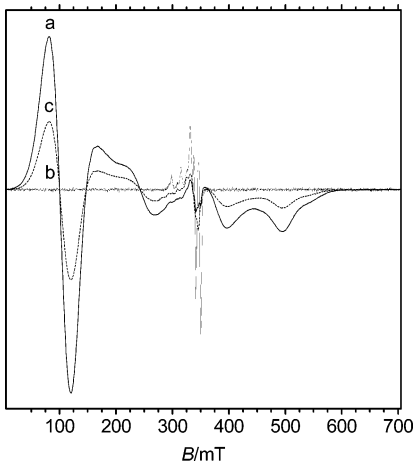

Figure 8. One-electron reduction and reoxidation of **1** in CH_2Cl_2 + 0.1 M TBAP under argon at 10 K. Initial state (a): concentration ca. 7.8 mM; microwave frequency, 9.65401 GHz; microwave power, 0.80 mW; modulation frequency, 100 kHz; modulation amplitude, 1.04 mT; one scan, 336 s. One-electron reduction (b): same parameters except concentration ca. 10 mM; microwave frequency, 9.65484 GHz; microwave power, 3.2 μW. One-electron reoxidation (c): same parameters as (a) except concentration ca. 7.6 mM; microwave frequency, 9.65544 GHz. Intensities were normalized for comparison, taken into account temperature, microwave power, gain, concentration, and saturation effects.

intensity in the final EPR signal, it is seen that the initial dicopper(II,II) species is not quantitatively restored,[43] as previously observed by UV−vis spectroscopy.

Mixed-valent compounds have been classified into three groups,[7] depending on whether an unpaired electron is completely localized (type I), partially delocalized (type II), or fully delocalized (type III). The Cu_A center is one of the few examples of type III dinuclear copper complexes. In the course of the reduction of **1**, we observe the progressive decrease in the intensities of the UV−vis features at 352 and 592 nm (Figure 7). In addition, no band is observed in the visible/near-IR region. Such bands corresponding to intervalence transitions are observed for type II or type III mixed-valent compounds. Therefore, the valence-localized species in this case can be considered to be type I rather than type II mixed-valent state.

Conclusion

The controlled preparation of a bis(μ-thiolato) dicopper-(II) complex (**1**) has been achieved using a new sterically bulky ligand with mixed N, S(thioether), and S(thiolate) donors. Herein, the overall multifrequency EPR studies unambiguously show that the observed EPR signals can be interpreted as a triplet state signal even if the isotropic spin−spin coupling is weak. Combined EPR experiments for **1** have provided a precise determination of the spin Hamiltonian parameters with a non-negligible axial zero-field splitting. In contrast, the three related bis(μ-thiolato)dicopper-(II,II) compounds[16−18] reported, display no EPR signal.

After the one-electron reduction of **1,** significant changes are observed in the EPR spectra of the solution. It displays a four-line hyperfine structure, indicating a type I, trapped valent state (Figure 8b), as observed at pH = 4.0 for an engineered Cu_A center in azurin.[14] The presence of a short Cu···Cu distance (∼2.4−2.9 Å), as for the Cu_A site in C*cO* [1,2,13] and the active site in N_2OR[4] appears to be characteristic of type III $Cu^{1.5}Cu^{1.5}$ centers.[44]

Furthermore, as postulated in the Cu_A center[8,45] or in models[46,47] coordination number along to geometric features (a near planarity of Cu_2S_2 core unit...) may be important requirements for access and reversibility of the $Cu^{II}Cu^{II}/Cu^{II}$-Cu^{I} and $Cu^{II}Cu^{I}/Cu^{I}Cu^{I}$ couples. These features lead to minimal structural reorganization that accompanies and facilitates the redox behavior. The related $Cu^{II}Cu^{II}$ complexes[16,17] do not allow the preparation of the corresponding mixed-valent bis(μ-thiolato)dicopper(II,I) complexes. In contrast, reversible interconversion between **1** and the corresponding one-electron electrogenerated localized mixed-valent species (type I) has been supported by EPR, UV−vis, and electrochemistry.

For **1**, these behaviors could be associated to structural features as the almost planar Cu_2S_2 core and the long Cu···Cu distance (3.418(8) Å) evidenced by the X-ray study.

Experimental Section

General. All reagents were purchased from commercial sources and used as received. Solvents were purified by standard methods before use. ***Caution:*** *Although no problems were encountered, suitable care and precautions should be taken when handling the perchlorate salts.*

Physical Measurements. UV−vis spectra were obtained using a Perkin-Elmer Lambda 2 spectrophotometer operating in the 200−1100 nm range with quartz cells. Temperature was maintained at 25 °C with a temperature control unit. ε values are given in M^{-1} cm^{-1} and are estimated on the basis of a linear regression. The calculated errors on the estimated values are of c.a. 3%. ^1H NMR spectra were recorded on a Bruker Advance 300 spectrometer at 25 °C with the deuterated solvent as lock.

Synthesis. *N*-((2-*tert*-Butyl-thiobenzyl)-*N*-(2-cyanoethylthiobenzyl)-*N*-(2-pyridylmethyl))amine (4). A solution of **3**[21] (3.4 g, 12 mmol) in dry methanol (100 mL) containing glacial acetic acid (2.9 mL, 80 mmol) was added to a solution of 2-(*tert*-butylthio)benzaldehyde (2.9 g, 14.9 mmol) in 50 mL of dry methanol. $NaBH_3CN$ (3.2 g, 80 mmol) was added to the reaction mixture under nitrogen atmosphere, and the suspension was stirred for 24 h. After this period, the pH of the ice-cold reaction mixture was adjusted to 2.0 by careful addition of concentrated HCl, and the mixture was stirred for an additional hour. The solution was reduced to dryness under reduced pressure, and the resulting residue was redissolved in 30 mL of water. The aqueous solution was washed two times with dichloromethane, and the pH of the solution was then adjusted to about 8 by addition of $NaHCO_3$. The resulting slightly basic solution was then extracted four times with dichlo-

(43) The signals around $g = 2$ (uncoupled dicopper(II,II), mononuclear Cu^{II}, or remaining dicopper(II,I) components) display higher intensity compared to the initial state (spectrum a). Quantitative analysis has been tempted but without success. Moreover, Cu^{II}-type component corresponds to an overlap of at least three spectra: a broad line due to the $S = 1$ and at least two Cu^{II}-type spectra.

(44) Gupta, R.; Zhang, Z. H.; Powell, D.; Hendrich, M. P.; Borovik, A. S. *Inorg. Chem.* **2002**, *41*, 5100−5106.
(45) Randall, D. W.; Gamelin, D. G.; LaCroix, L. B.; Solomon, E. I. *J. Biol. Inorg. Chem.* **2000**, *5*, 16−19.
(46) Osako, T.; Ueno, Y.; Tachi, Y.; Itoh, S. *Inorg. Chem.* **2003**, *42*, 8087−8097.
(47) Harkins, S. B.; Peters, J. C. *J. Am. Chem. Soc.* **2004**, *126*, 2885−2893.

romethane. The extracts were combined, washed with brine, and dried over anhydrous Na_2SO_4. The solvent was removed in vacuo to give the crude product as a brown oil. The latter was purified by chromatography on silica gel and eluted with ethyl acetate/cyclohexane (1:3, v/v) to give (3.6 g, 7.8 mmol, 65% yield) of **4** as a yellow oil. ^{1}H NMR (300 MHz, $CDCl_3$, 25 °C, TMS): δ 8.48 (d, ^3J(H,H) = 4.4 Hz, 1H; Py−*H1*), 7.75−7.08 (m, 11H; Ar−*H*), 3,97 (s, 2H; NC*H*$_2$Py), 3.81 (s, 2H; NC*H*$_2$Ar*StBu*), 3.75 (s, 2H; NC*H*$_2$ArSCH$_2$−), 3.05 (t, ^3J(H,H) = 7.3 Hz, 2H; −C*H*$_2$CN), 2.50 (t, ^3J(H,H) = 7.3 Hz, 2H; SC*H*$_2$-), 1.20 (s, 9H, S(C*H*$_3$)$_3$); ^{13}C NMR (75,465 MHz, $CDCl_3$, 25 °C,) δ 160.0, 148.9, 144.4, 141.0, 139.0, 136.5, 133.6, 132.8, 130.8, 130.6, 130.1, 129.1, 127.9, 127.5, 126.9, 123.4, 122.1, 118.2, 60.5, 57.0, 56.9, 47.4, 31.3, 30.0, 18.2; MS (CI, NH_3 + isobutane), *m*/*z* (%): 462 (100) $[M + H]^+$; elemental analysis calcd (%) for $C_{27}H_{31}N_3S_2$ (461): C 70.24, H 6.77, N 9.10, S 13.89; found: C 69.89, H 6.72, N 8.94, S 13.67.

***N*-((2-Mercaptobenzyl)-*N*-(2-cyanoethylthiobenzyl)-*N*-(2-pyridylmethyl))amine [N$_2$SS′H].** Under argon, Na (0.13 g, 5.6 mmol) was slowly added to ice-bath-cooled methanol (40 mL). Stirring was continued for an additional 10 min before dropwise addition of **4** (0.32 g, 0.7 mmol) in methanol (15 mL). The reaction mixture was stirred for 5 h at 50 °C. After addition of an excess of $NaBH_4$ (0.27 g, 7 mmol), the mixture was poured onto ice and a saturated solution of NH_4Cl was added to achieve pH ≈ 5 followed by Et_2O extraction (3 × 50 mL). The Et_2O extracts were washed with saturated aqueous NaCl and dried over anhydrous Na_2SO_4. After filtration, the solvent was removed in vacuo to give [N$_2$SS′H] as a pale yellow oil (0.28 g, 0.689 mmol, 98%) used without any further purification. ^{1}H NMR (300 MHz, $CDCl_3$, 25 °C,) δ 8.51 (d, ^3J(H,H) = 4.6 Hz, 1H; Py−*H1*), 7.78 (dt, ^3J(H,H) = 7.8 Hz, ^3J(H,H) = 7.6 Hz, 1H; Py−*H4*,), 7.69 (dd, ^3J(H,H) = 7.6 Hz, 1H; ArSH−*H1*), 7.56 (dd, ^3J(H,H) = 7.5 Hz, 1H; Py−*H3*), 7.52 (d, ^3J(H,H) = 7.8 Hz, 1H; ArS*tBu*−*H4*,), 7.41 (dt, ^3J(H,H) = 7.4 Hz, 1H; ArSH−*H2*,), 7.35−7.30 (m, 3H; Ar−*H*), 7.22 (dd, ^3J(H,H) = 6.8 Hz, 1H, ArS*tBu*−*H2*,), 7.08 (dt, ^3J(H,H) = 6.2 Hz, ^3J(H,H) = 7.5 Hz, 1H; ArSH−*H4*), 6.98 (dt, ^3J(H,H) = 7.5 Hz, ^3J(H,H) = 7.3 Hz, 1H; ArS*tBu*−*H1*,), 4.32 (s, 2H; NC*H*$_2$Py), 4.04 (s, 2H; NC*H*$_2$Ar*StBu*), 3.96 (s, 2H; NC*H*$_2$ArSH), 1.14 (s, 9H; S(C*H*$_3$)$_3$); ^{13}C NMR (CD_3-OD): δ 157.3, 150.5, 143.4, 141.6, 141.2, 139.4, 135.9, 134.9, 134.4, 133.9, 133.0, 131.2, 130.5, 130.3, 127.1, 125.3, 125.1, 61.5, 60.0, 58.9, 47.8, 32.1; MS (CI, NH_3 + isobutane), *m*/*z* (%): 408 (100) $[M^+]$. Treatment of [N$_2$SS′H] with 1 M HCl in dichloromethane, addition of Et_2O, and cooling at −20 °C gave a white solid of [N$_2$SS′H] ·2HCl; elemental analysis calcd for $C_{24}H_{28}N_2S_2$·2HCl (481.5) C 59.86, H 6.28, N 5.82; found: C 59.62, H 6.17, N 5.83.

[Cu$_2$(N$_2$SS′)$_2$](ClO$_4$)$_2$·C$_4$H$_{10}$O (1). To a solution of [N$_2$SS′H] (200 mg, 0.49 mmol) in distilled methanol (20 mL) under argon was added slowly a solution of $Cu(ClO_4)_2$·$6H_2O$ (185 mg, 0.49 mmol) in methanol (10 mL). The dark solution was stirred for 1 h at room temperature, and diethyl ether (20 mL) was added. After 12 h at −20 °C, the crude product precipitated. A black powder was recovered after filtration (350 mg, 0.3 mmol, 63%). Recrystallization by vapor diffusion of diethyl ether into a methanol solution of this solid afforded after 24 h black-purple crystals of **1** suitable for X-ray diffraction. Elemental analysis calcd (%) for $C_{48}H_{54}N_4O_8Cl_2S_4Cu_2$ (1141): C 50.52, H 4.77, N 4.91, Cu 11.14; found: C 50.18, H 4.83, N 4.96, Cu, 11.00; MS (ESI), *m*/*z* (%): 1040.8 (100) $[Cu_2(N_2SS')_2(ClO_4)^+]$, 470.0 (40) $[Cu_2(N_2SS')_2^{2+}]$; UV−vis (dichloromethane), λ_{max}, nm (ϵ, M^{-1} cm^{-1})): 350(7158), 592 (1204).

EPR Spectroscopy. X-band EPR spectra were recorded on a Bruker EMX, with an Oxford Instruments ESR-900 continuous-flow helium cryostat and an ER-4116 DM Bruker cavity. Q-band EPR spectra were recorded on a Bruker ESP 300 E, with an Oxford Instruments CF-935 continuous-flow helium cryostat and an ER-5106 QT Bruker cavity. One hundred fifteen gigahertz EPR spectra were recorded on a laboratory-made spectrometer.[48,49] A gun diode operating at 115 GHz was used as the radiation source. The magnetic field was produced by a superconducting magnet (0−12 T). The simulations of a 2(S = 1/2) and an S = 1 systems have been perform with a MATLAD code: EasySpin version 2.5.1 (2006)[50] using exact diagonalization of the 4 × 4 (two spin 1/2) and 3 × 3 (one spin 1) matrices. The intensity of each transition has been taken in to account.

Electrochemistry. The electrochemical behavior of millimolar solutions of **1** was investigated in 0.1 M tetra-*n*-butylammonium perchlorate (TBAP) in CH_2Cl_2 using a EGG 273 Potentiostat coupled with a Kipp&Zonen $x-y$ recorder. The experiments were performed in a three-compartment cell, at room temperature, under argon atmosphere. Potentials are referred to an Ag/10 mM $AgNO_3$ + CH_3CN + 0.1 M TBAP reference electrode (+0.07 V vs ferrocene/ferrocinium used as an internal reference). The working electrode was a platinum disk of 5 mm diameter for the cyclic voltammetry (CV, 0.1 V s^{-1}) experiments or 2 mm diameter for the rotating disk electrode (RDE, 600 rpm) voltammetry experiments. The working electrode was polished with 1 μm diamond paste prior to each record. Electrolysis was performed at 0 °C.

Crystallography. Crystal data for **1** were collected at 293 K on a Bruker-Nonius kappa CCD diffractometer using graphite-monochromated Mo Kα radiation (λ = 0.71073 Å). A dark purple platelet (0.18 × 0.14 × 0.09 mm^3) was glue-mounted on the tip of a glass fiber.

Data: M_l = 1141.22, orthorhombic, space group *Pbcn*, a = 10.627(1) Å, b = 23.776(1) Å, c = 22.477(2) Å, V = 5679(1) $Å^3$, Z = 4, ρ_{calcd} = 1.424 Mg m^{-3}, μ = 0.7107 cm^{-1}, observed data: 4822, R1: 0.0651, wR2: 0.0673, $R1 = \sum||F_o| - |F_c||/\sum|F_o|$, $wR2 = [\sum(|F_o| - |F_c|)^2/\Sigma wF_o^2]^{1/2}]$ with $w = 1/[\sigma^2(F_o) + p|F_o|^2]$. The structure was solved using SIR92, and the refinement was done on F using the TeXsan software package.[51] No absorption correction was done. All non-hydrogen atoms were refined anisotropically. Hydrogen atoms were generated in idealized positions, riding on the carrier atoms with isotropic thermal parameters. CCDC-274886 contains the full data collection parameters and structural data for **1**.

Acknowledgment. The authors are grateful to Dr J.-M. Latour for his contribution to this work. They thank Dr. S. Gambarelli and Dr. J. -M. Mouesca for helpful discussions, G. Desfond for EPR technical support, and C. Lebrun for ESI mass measurements.

Supporting Information Available: Listing of ESI-MS, solid-state X- and Q-band EPR for **1**, resonant magnetic field as a function of D for X-band, comparison of the simulations of an S = 1 and a 2(S = 1/2) systems at X-, Q-, and F-band frequencies in PDF format, and X-ray crystallographic file for **1** in CIF format. This material is available free of charge via the Internet at http://pubs.acs.org.

IC0612606

(48) Barra, A. L.; Brunel, L. C.; Robert, J. B. *Chem. Phys. Lett.* **1990**, *165*, 107−109.
(49) Muller, F.; Hopkins, M. A.; Coron, N.; Grynderg, M.; Brunel, L. C.; Martinez, G. *Rev. Sci. Instrum.* **1989**, *60*, 3681−3684.
(50) Stoll, S.; Schweiger, A. *J. Magn. Reson.* **2006**, *178*, 42−55.
(51) *TEXsan*, version 1.7; Molecular Structure Corporation: The Woodlands, TX, 1995.